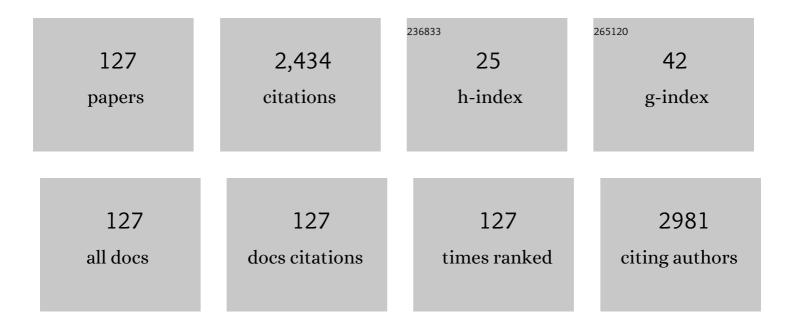
Chung-Kwei Lin

List of Publications by Year in descending order

Source: https://exaly.com/author-pdf/9558073/publications.pdf Version: 2024-02-01



#	Article	IF	CITATIONS
1	Effect of progressive muscle relaxation on postoperative pain, fatigue, and vital signs in patients with head and neck cancers: A randomized controlled trial. Patient Education and Counseling, 2022, 105, 2151-2157.	1.0	10
2	Impact of Zr-Doped Bi2O3 Radiopacifier by Spray Pyrolysis on Mineral Trioxide Aggregate. Materials, 2021, 14, 453.	1.3	2
3	Mesoporous Properties of Bioactive Glass Synthesized by Spray Pyrolysis with Various Polyethylene Glycol and Acid Additions. Polymers, 2021, 13, 618.	2.0	7
4	Bonding and Thermal Cycling Performances of Two (Poly)Aryl–Ether–Ketone (PAEKs) Materials to an Acrylic Denture Base Resin. Polymers, 2021, 13, 543.	2.0	8
5	Hard Anodization Film on Carbon Steel Surface by Thermal Spray and Anodization Methods. Materials, 2021, 14, 3580.	1.3	3
6	A Novel Sol-Gel Bi2-xHfxO3+x/2 Radiopacifier for Mineral Trioxide Aggregates (MTA) as Dental Filling Materials. Applied Sciences (Switzerland), 2021, 11, 7292.	1.3	3
7	Hydrothermal Synthesis of Co ₃ O ₄ /ZnCo ₂ O ₄ Core-Shell Nanostructures for High-Performance Supercapacitors. Journal of the Electrochemical Society, 2021, 168, 123502.	1.3	5
8	Effect of Tantalum Pentoxide Addition on the Radiopacity Performance of Bi2O3/Ta2O5 Composite Powders Prepared by Mechanical Milling. Materials, 2021, 14, 7447.	1.3	3
9	Additive manufacturing of dental prosthesis using pristine and recycled zirconia solvent-based slurry stereolithography. Ceramics International, 2020, 46, 28701-28709.	2.3	20
10	The Design of ZnO Nanorod Arrays Coated with MnOx for High Electrochemical Stability of a Pseudocapacitor Electrode. Nanomaterials, 2020, 10, 475.	1.9	18
11	Effects of Milling Time, Zirconia Addition, and Storage Environment on the Radiopacity Performance of Mechanically Milled Bi2O3/ZrO2 Composite Powders. Materials, 2020, 13, 563.	1.3	12
12	Electrochemistry and Rapid Electrochromism Control of MoO3/V2O5 Hybrid Nanobilayers. Materials, 2019, 12, 2475.	1.3	21
13	Microstructure of Iron (Fe) Nanowires Synthesized by Chemical Reduction of Different Fe Ionic Precursors. Microscopy and Microanalysis, 2019, 25, 2232-2233.	0.2	0
14	Effect of Oxygen Concentration and Tantalum Addition on the Formation of High Temperature Bismuth Oxide Phase by Mechanochemical Reaction. Materials, 2019, 12, 1947.	1.3	5
15	Spherical Composite Powder by Coupling Polymethyl Methacrylate and Boron Nitride via Spray Drying for Cosmetic Application. Materials, 2019, 12, 706.	1.3	7
16	Sintering Pmperature-Dependence on Radiopacity of Bi(2â^'x) ZrxO(3+x/2) Powders Prepared by Sol-Gel Process. Materials, 2018, 11, 1685.	1.3	14
17	Effect of Hydroxyapatite Formation on Titanium Surface with Bone Morphogenetic Protein-2 Loading through Electrochemical Deposition on MG-63 Cells. Materials, 2018, 11, 1897.	1.3	18
18	Low operating temperature CO sensor prepared using SnO2 nanoparticles. Journal of Electroceramics, 2018, 41, 28-36.	0.8	6

#	Article	IF	CITATIONS
19	Effect of (Ti, Al)N Nanostructured Arc-Coatings on Wear and Corrosion Properties of 4340 Alloy Steel. Journal of Nanoscience and Nanotechnology, 2018, 18, 2823-2829.	0.9	0
20	Radiopacity performances of precipitated ZrO2-doped Bi2O3 powders and the influences of dopant concentrations and sintering temperatures. Ceramics International, 2017, 43, 14008-14014.	2.3	9
21	Characterization of bioactive glassâ€coated carbon nanotubes prepared by solgel process. International Journal of Applied Glass Science, 2017, 8, 239-246.	1.0	4
22	Growth factors-loaded calcium phosphate/polymer hybrid coating with sequential release behavior prepared via electrochemical deposition method. Surface and Coatings Technology, 2016, 303, 237-243.	2.2	4
23	Preparation and characterization of silver nanocrystals decorated mesoporous bioactive glass via synchrotron X-ray reduction. Journal of Non-Crystalline Solids, 2016, 450, 128-134.	1.5	7
24	Hydrophilic/hydrophobic surface of Al 2 O 3 thin films grown by thermal and plasma-enhanced atomic layer deposition on plasticized polyvinyl chloride (PVC). Surface and Coatings Technology, 2016, 305, 158-164.	2.2	35
25	Anode Catalyst of Hybrid AuPd and Rare Earth Doped Cerium Oxide/Multi-Walled Carbon Nanotubes for Direct Formic Acid Fuel Cells. Funtai Oyobi Fummatsu Yakin/Journal of the Japan Society of Powder and Powder Metallurgy, 2016, 63, 706-713.	0.1	2
26	Effects of adding different morphological carbon nanomaterials on supercapacitive performance of sol–gel manganese oxide films. Ceramics International, 2016, 42, 4797-4805.	2.3	11
27	Thermoelectric Properties of Alumina-Doped Bi0.4Sb1.6Te3 Nanocomposites Prepared through Mechanical Alloying and Vacuum Hot Pressing. Energies, 2015, 8, 12573-12583.	1.6	14
28	X-ray irradiation synthesis of PEG-coated Au-Pd nanoparticles. Nanotechnology, 2015, 26, 355601.	1.3	2
29	Uncapped Au–Pd colloidal nanoparticles show catalytic enhancement. RSC Advances, 2015, 5, 61846-61850.	1.7	2
30	Influence of Fe3O4 nanoparticles on pseudocapacitive behavior of the charge storage process. Journal of Alloys and Compounds, 2015, 645, 250-258.	2.8	9
31	Photocatalyst ZnO-doped Bi2O3 powder prepared by spray pyrolysis. Powder Technology, 2015, 272, 316-321.	2.1	16
32	A study on the corrosion and erosion behavior of electroless nickel and TiAlN/ZrN duplex coatings on ductile iron. Applied Surface Science, 2015, 324, 13-19.	3.1	26
33	Radiopacity and Cytotoxicity of Portland Cement Containing Zirconia Doped Bismuth Oxide Radiopacifiers. Journal of Endodontics, 2014, 40, 251-254.	1.4	19
34	Large-area TiO2 nanotube dye-sensitized solar cells using thermal-sprayed Ti layers on stainless steel. Ceramics International, 2014, 40, 3221-3226.	2.3	6
35	The optical properties and sunscreen application of spherical h-BN–TiO2/mica composite powder. Ceramics International, 2014, 40, 4691-4696.	2.3	16
36	Cosmetic properties of TiO2/mica-BN composite powder prepared by spray drying. Ceramics International, 2014, 40, 6903-6911.	2.3	30

#	Article	IF	CITATIONS
37	Electrochromic properties of nanostructured tungsten oxide films prepared by surfactant-assisted sol–gel process. Surface and Coatings Technology, 2013, 231, 403-407.	2.2	31
38	Annealing induced structural evolution and electrochromic properties of nanostructured tungsten oxide films. Thin Solid Films, 2013, 549, 258-262.	0.8	13
39	High supercapacitive performance of sol–gel ZnO-doped manganese oxide coatings. Thin Solid Films, 2013, 528, 61-66.	0.8	13
40	Hierarchical ZnO nanorod-array films with enhanced photocatalytic performance. Thin Solid Films, 2013, 528, 167-174.	0.8	44
41	Template assisted fabrication of TiO 2 and WO 3 nanotubes. Ceramics International, 2013, 39, 6631-6636.	2.3	20
42	Enhanced efficiency in In <scp>G</scp> a <scp>N</scp> â€based photovoltaic devices combined with nanocrystalline Bi ₂ <scp>O</scp> ₃ / <scp>P</scp> 3 <scp>HT</scp> heterojunction structures. Physica Status Solidi (A) Applications and Materials Science, 2013, 210, 1133-1136.	0.8	4
43	The Effects of Size and Shape of Iron Particles on the Microwave Absorbing Properties of Composite Absorbers. IEEE Transactions on Magnetics, 2013, 49, 4180-4183.	1.2	22
44	Characterization of electrochromic tungsten oxide film from electrochemical anodized RF-sputtered tungsten films. Ceramics International, 2013, 39, 4293-4298.	2.3	24
45	Improved pseudo-capacitive performance of manganese oxide films synthesized by the facile sol–gel method with iron acetate addition. Ceramics International, 2013, 39, 7831-7838.	2.3	11
46	Synthesis and characterization of electrochromic plate-like tungsten oxide films by acidic treatment of electrochemical anodized tungsten. Electrochimica Acta, 2013, 112, 24-31.	2.6	27
47	Effect of electroless nickel interlayer on wear behavior of CrN/ZrN multilayer films on Cu-alloyed ductile iron. Applied Surface Science, 2013, 284, 59-65.	3.1	17
48	High supercapacitive stability of spray pyrolyzed ZnO-added manganese oxide coatings. Ceramics International, 2013, 39, 1885-1892.	2.3	10
49	Functionalized polymer spheres via one-step photoinduced synthesis for antimicrobial activity and gene delivery. Nanotechnology, 2012, 23, 255103.	1.3	9
50	Nanostructured Na-doped vanadium oxide synthesized using an anodic deposition technique for supercapacitor applications. Journal of Alloys and Compounds, 2012, 536, S428-S431.	2.8	27
51	Effect of iron particle addition on the pseudocapacitive performance of sol–gel derived manganese oxides film. Materials Chemistry and Physics, 2012, 137, 503-510.	2.0	9
52	Structural evolution and chemical bonds in electrochromic WO ₃ films during electrochemical cycles. Journal Physics D: Applied Physics, 2012, 45, 225303.	1.3	25
53	Non-catalytic and substrate-free method to titania-doped W18O49 nanorods: growth, characterizations, and electro-optical properties. Journal of Nanoparticle Research, 2012, 14, 1.	0.8	5
54	Mechanical behavior of TiN/CrN nano-multilayer thin film deposited by unbalanced magnetron sputter process. Journal of Alloys and Compounds, 2011, 509, 3197-3201.	2.8	32

#	Article	IF	CITATIONS
55	A facile route to tungsten oxide nanomaterials with controlled morphology and structure. Particuology, 2011, 9, 517-521.	2.0	4
56	Microwave absorbing properties of iron nanowire at x-band frequencies. Journal of Applied Physics, 2011, 109, .	1.1	30
57	Electrochromic performance of hybrid tungsten oxide films with multiwalled-CNT additions. Thin Solid Films, 2011, 520, 1375-1378.	0.8	20
58	Gas sensors with porous three-dimensional framework using TiO2/polymer double-shell hollow microsphere. Thin Solid Films, 2011, 520, 1546-1553.	0.8	24
59	High-yield fabrication of W18O49@TiO2 core–shell nanoparticles: microstructures and optical-thermal properties. Journal of Nanoparticle Research, 2011, 13, 4549-4555.	0.8	4
60	Bias effects on microstructure, mechanical properties and corrosion resistance of arc-evaporated CrTiAlN nanocomposite films on AISI 304 stainless steel. Thin Solid Films, 2011, 519, 4928-4932.	0.8	10
61	The Effect of Processing Parameters on the Synthesis of Tungsten Oxide Nanomaterials by a Modified Plasma Arc Gas Condensation Technique. Journal of Nanoscience and Nanotechnology, 2010, 10, 5461-5466.	0.9	5
62	Structural Investigations of Hybrid TiO ₂ /CNTs Nanomaterials. Journal of Nanoscience and Nanotechnology, 2010, 10, 3155-3161.	0.9	5
63	Manganese oxide thin films prepared by potentiodynamic electrodeposition and their supercapacitor performance. Journal of Solid State Electrochemistry, 2010, 14, 1697-1703.	1.2	19
64	Structure and optical properties of tungsten oxide nanomaterials prepared by a modified plasma arc gas condensation technique. Journal of Nanoparticle Research, 2010, 12, 1755-1763.	0.8	18
65	Bias effects on the tribological behavior of cathodic arc evaporated CrTiAlN coatings on AISI 304 stainless steel. Thin Solid Films, 2010, 518, 3825-3829.	0.8	30
66	Analysis on microstructure and characteristics of TiAlN/CrN nano-multilayer films deposited by cathodic arc deposition. Thin Solid Films, 2010, 518, 7519-7522.	0.8	25
67	Selective growth of ZnO nanorods for gas sensors using ink-jet printing and hydrothermal processes. Thin Solid Films, 2010, 519, 1693-1698.	0.8	71
68	Microstructural and optical properties of Ga-doped ZnO semiconductor thin films prepared by sol–gel process. Thin Solid Films, 2010, 519, 1516-1520.	0.8	98
69	Transparent semiconductor zinc oxide thin films deposited on glass substrates by sol–gel process. Ceramics International, 2010, 36, 1791-1795.	2.3	78
70	Magnetoelectric behavior of carbonyl iron mixed Mn oxide-coated ferrite nanoparticles. Journal of Applied Physics, 2010, 107, 09D904.	1.1	3
71	Fabrication and corrosion behavior of Ti-based bulk metallic glass composites containing carbon nanotubes. Journal of Alloys and Compounds, 2010, 504, S176-S179.	2.8	4
72	Fabrication and optical properties of Ti-doped W18O49 nanorods using a modified plasma-arc gas-condensation technique. Journal of Vacuum Science & Technology B, 2009, 27, 2170-2174.	1.3	27

#	Article	IF	CITATIONS
73	The properties of transparent semiconductor Zn1â^'Ti O thin films prepared by the sol–gel method. Thin Solid Films, 2009, 518, 1603-1606.	0.8	34
74	Hybrid manganese oxide films for supercapacitor application prepared by sol–gel technique. Thin Solid Films, 2009, 518, 1557-1560.	0.8	26
75	Electrophoretically deposited manganese oxide coatings for supercapacitor application. Ceramics International, 2009, 35, 3469-3474.	2.3	19
76	Pseudocapacitive properties of carbon nanotube/manganese oxide electrode deposited by electrophoretic deposition. Diamond and Related Materials, 2009, 18, 482-485.	1.8	18
77	Tungsten Oxide Nanopowders and Nanorods Prepared by a Modified Plasma Arc Gas Condensation Technique. Materials Transactions, 2009, 50, 2593-2597.	0.4	9
78	Supercapacitive properties of spray pyrolyzed iron-added manganese oxide powders deposited by electrophoretic deposition technique. Thin Solid Films, 2008, 517, 1234-1238.	0.8	16
79	Formation of Irregular Nanocrystalline CeO2 Particles from Acetate-Based Precursor via Spray Pyrolysis. Journal of Materials Engineering and Performance, 2008, 17, 20-24.	1.2	13
80	In situ X-ray absorption spectroscopic studies of anodically deposited binary Mn–Fe mixed oxides with relevance to pseudocapacitance. Journal of Power Sources, 2008, 178, 476-482.	4.0	23
81	Characterization of nanocrystalline manganese oxide powder prepared by inert gas condensation. Ceramics International, 2008, 34, 1661-1666.	2.3	7
82	Investigation of the microstructure and characterizations of TiN/CrN nanomultilayer deposited by unbalanced magnetron sputter process. Surface and Coatings Technology, 2008, 203, 657-660.	2.2	26
83	Photocatalytic properties of porous TiO2/Ag thin films. Thin Solid Films, 2008, 516, 1743-1747.	0.8	48
84	Effect of Sn-doped on microstructural and optical properties of ZnO thin films deposited by sol–gel method. Thin Solid Films, 2008, 517, 1032-1036.	0.8	209
85	Oxygen partial pressure effect on the preparation of nanocrystalline tungsten oxide powders by a plasma arc gas condensation technique. International Journal of Refractory Metals and Hard Materials, 2008, 26, 423-428.	1.7	19
86	Hydrogen Absorption Performance of Mechanically Alloyed (Mg ₂ Ni) _{100−<i>x</i>} Ti <i>_x</i> Powder. Materials Transactions, 2007, 48, 3170-3175.	0.4	3
87	Improvement of Hydrogen Absorption Performances of Mechanically Alloyed Mg ₂ Ni Powders by Water Cooling. Materials Transactions, 2007, 48, 842-846.	0.4	3
88	Preparation and Characterization of Dual-Phase Bulk Metallic Glasses through Powder Metallurgy Route. Materials Transactions, 2007, 48, 1595-1599.	0.4	2
89	Formation of tungsten oxide encapsulated in titanium oxide nanocages by modified plasma arc gas condensation. Nanotechnology, 2007, 18, 155602.	1.3	7
90	Manganese oxide films prepared by sol–gel process for supercapacitor application. Surface and Coatings Technology, 2007, 202, 1272-1276.	2.2	88

#	Article	IF	CITATIONS
91	Performance of sol–gel deposited Zn1â^'xMgxO films used as active channel layer for thin-film transistors. Surface and Coatings Technology, 2007, 202, 1323-1328.	2.2	29
92	Characterization of spray pyrolyzed manganese oxide powders deposited by electrophoretic deposition technique. Surface and Coatings Technology, 2007, 202, 1277-1281.	2.2	38
93	Low temperature sintering and magnetic properties of garnet microwave magnetic materials. Materials Chemistry and Physics, 2007, 105, 408-413.	2.0	9
94	A novel method of supporting gold nanoparticles on MWCNTs: Synchrotron X-ray reduction. Particuology: Science and Technology of Particles, 2007, 5, 237-241.	0.4	5
95	The effect on the microstructures of electroless nickel coatings initiated by pulsating electric current. Thin Solid Films, 2007, 516, 355-359.	0.8	3
96	Improvement in the characteristics of GaN-based light-emitting diodes by inserting AlGaN-GaN short-period superlattices in GaN underlayers. IEEE Photonics Technology Letters, 2006, 18, 1497-1499.	1.3	7
97	Formation and characterization of mechanically alloyed Ti–Cu–Ni–Sn bulk metallic glass composites. Intermetallics, 2006, 14, 957-961.	1.8	17
98	Influence of the trench depths of grooved GaN templates on the characteristics of overgrown AlGaN films. Journal of Crystal Growth, 2006, 297, 339-344.	0.7	0
99	On the characteristics of AlGaN films grown on (111) and (001) Si substrates. Solid State Communications, 2006, 137, 63-66.	0.9	2
100	Characterization of elecrophoretically deposited nanocrystalline titanium dioxide films. Surface and Coatings Technology, 2006, 200, 3184-3189.	2.2	43
101	Polymerization-like grafting of thermoplastic polyurethane by microwave plasma treatment. Surface and Coatings Technology, 2006, 200, 3380-3384.	2.2	14
102	The failure mechanism of diamond like coatings prepared by the filtered cathodic arc technique for minting application. Surface and Coatings Technology, 2006, 201, 4430-4435.	2.2	5
103	Preparation and characterization of nanocrystalline porous TiO2/WO3 composite thin films. Thin Solid Films, 2006, 494, 228-233.	0.8	33
104	Photocatalytic properties of nanocrystalline TiO2 thin film with Ag additions. Thin Solid Films, 2006, 494, 274-278.	0.8	58
105	A Modified Plasma Arc Gas Condensation Technique to Synthesize Nanocrystalline Tungsten Oxide Powders. Materials Transactions, 2005, 46, 1016-1020.	0.4	13
106	Deposition of AlGaN films on (111) Si substrates and optimization of GaN growth on Si using intermediate-temperature AlGaN buffer layers. Thin Solid Films, 2005, 493, 135-138.	0.8	1
107	A study of nanoparticle manufacturing process using vacuum submerged arc machining with aid of enhanced ultrasonic vibration. Journal of Materials Science, 2005, 40, 1005-1010.	1.7	13
108	Characterization of Ni57Zr20Ti18Al5 amorphous powder obtained by mechanical alloying. Materials Chemistry and Physics, 2004, 84, 358-362.	2.0	6

#	Article	IF	CITATIONS
109	Process development of a novel arc spray nanoparticle synthesis system (ASNSS) for preparation of a TiO 2 nanoparticle suspension. International Journal of Advanced Manufacturing Technology, 2004, 24, 879-885.	1.5	12
110	Preparation and thermal stability of mechanically alloyed amorphous Ni–Zr–Ti–Si composites. Materials Science & Engineering A: Structural Materials: Properties, Microstructure and Processing, 2004, 375-377, 820-824.	2.6	5
111	Preparation and thermal stability of mechanically alloyed Ni–Zr–Ti–Y amorphous powders. Intermetallics, 2004, 12, 1011-1017.	1.8	7
112	TiO ₂ Nanoparticle Suspension Preparation Using Ultrasonic Vibration-Assisted Arc-Submerged Nanoparticle Synthesis System (ASNSS). Materials Transactions, 2004, 45, 806-811.	0.4	16
113	A Study of Magnetic Field Effect on Nanofluid Stability of CuO. Materials Transactions, 2004, 45, 1375-1378.	0.4	17
114	Consolidation of amorphous Ni–Zr–Ti–Si powders by vacuum hot-pressing method. Intermetallics, 2002, 10, 1277-1282.	1.8	34
115	Mechanical alloyed Ti–Cu–Ni–Si–B amorphous alloys with significant supercooled liquid region. Intermetallics, 2002, 10, 1271-1276.	1.8	12
116	Preparation and characterization of nanocrystalline Nb 3 Al alloy. Scripta Materialia, 2001, 44, 1967-1971.	2.6	2
117	Formation of NiAl–Al2O3 intermetallic-matrix composite powders by mechanical alloying technique. Intermetallics, 2000, 8, 1043-1048.	1.8	50
118	Preparation of iron nitride powders through mechanical alloying and atmospheric heat treatment. , 1999, , .		0
119	Acoustic emission studies on thermal spray materials. Surface and Coatings Technology, 1998, 102, 1-7.	2.2	22
120	Magnetic and structural properties of nanophase AgxFe1 â^' x solid solution particles. Scripta Materialia, 1998, 10, 457-464.	0.5	8
121	Amorphization reaction of Ni-Ta powders during mechanical alloying. Metallurgical and Materials Transactions A: Physical Metallurgy and Materials Science, 1997, 28, 1429-1435.	1.1	8
122	Acoustic emission responses of plasma-sprayed alumina-3% titania deposits. Thin Solid Films, 1997, 310, 108-114.	0.8	9
123	Elastic Response of Thermal Spray Deposits under Indentation Tests. Journal of the American Ceramic Society, 1997, 80, 2093-2099.	1.9	138
124	Acoustic Emission Studies of Aluminaâ€13% Titania Freeâ€Standing Forms during Fourâ€Point Bend Tests. Journal of the American Ceramic Society, 1997, 80, 2382-2394.	1.9	20
125	Simulation of Hardness Testing on Plasma-Sprayed Coatings. Journal of the American Ceramic Society, 1995, 78, 1406-1410.	1.9	11

126 CNTs stabilize high temperature anatase phase of TiO/sub 2/. , 0, , .

#	Article	IF	CITATIONS
127	Acoustic Emission Responses of Plasma Sprayed Ceramics During Four Point Bend Tests. Ceramic Engineering and Science Proceedings, 0, , 44-50.	0.1	5